

Control of the G-protein Cascade Dynamics by GDP Dissociation Inhibitors

Elena Nikonova¹, Mikhail A. Tsyganov², Walter Kolch^{1,3,4}, Dirk Fey^{1*} and Boris N. Kholodenko^{1,3,4*}

¹Systems Biology Ireland, University College Dublin, Belfield, Dublin 4, Ireland, ²Institute of Theoretical and Experimental Biophysics, Pushchino, Moscow Region, Russia, ³School of Medicine and Medical Science, University College Dublin, Belfield, Dublin 4, Ireland, ⁴Conway Institute of Biomolecular & Biomedical Research, University College Dublin, Belfield, Dublin 4, Ireland

* Corresponding authors: Boris N. Kholodenko (boris.kholodenko@ucd.ie), Dirk Fey (dirk.fey@ucd.ie)

Abstract

A network of the Rho family GTPases, which cycle between an inactive GDP-bound and active GTP-bound states, controls key cellular processes, including proliferation and migration. Activating and deactivating GTPase transitions are controlled by guanine nucleotide exchange factors (GEFs), GTPase activating proteins (GAPs) and GDP dissociation inhibitors (GDIs) that sequester GTPases from the membrane to the cytoplasm. Here we show that a cascade of two Rho family GTPases, RhoA and Rac1, regulated by RhoGDI1, exhibits distinct modes of the dynamic behavior, including abrupt, bistable switches, excitable overshoot transitions and oscillations. The RhoGDI1 abundance and signal-induced changes in the RhoGDI1 affinity for GTPases control these different dynamics, enabling transitions from a single stable steady state to bistability, to excitable pulses and to sustained oscillations of GTPase activities. These RhoGDI1-controlled dynamic modes of RhoA and Rac1 activities form the basis of cell migration behaviors, including protrusion-retraction cycles at the leading edge of migrating cells.

Introduction

Monomeric G proteins (small GTPases) control multiple cellular functions including cytoskeletal dynamics, transcriptional regulation, cell survival and vesicle trafficking.^{1,2} The GDP-bound form of a small GTPase is usually inactive, whereas a GTP-bound form is active. Active GTPases bind and stimulate downstream effector kinases and other proteins, thereby turning on key cellular responses, such as migration or mitogenesis. Constitutively active small GTPase mutants, such as mutant K-RasV12, are implicated in a variety of human cancers.³ In mammalian cells, GTPase activities are tightly controlled by several proteins that include (i) guanine nucleotide exchange factors (GEFs) that facilitate GDP/GTP exchange thereby activating GTPases, (ii) GTPase activating proteins (GAPs) that stimulate GTP hydrolysis and transition to the inactive GDP-bound state, and (iii) GDP dissociation inhibitors (GDIs) that bind GTPases, forcing them away from their effectors on the membrane and maintaining GTPases in an inactive form in the cytosol.⁴

Crosstalk between different GTPases is mediated by their effector proteins, which generate signaling networks where each GTPase may positively or negatively control multiple GEFs and GAPs.⁵⁻⁷ As a prototypic example, we will consider the two Rho-family GTPases, RhoA⁸ and Rac1, which together regulate cytoskeleton dynamics and cell motility.^{9,10} It was shown that during the protrusion-retraction process at the leading edge of migrating cells, RhoA activity is synchronized with the initial events of protrusion, whereas Rac1 activation is delayed.¹¹ This time lag of Rac1 activation and the fact that the RhoA effector mDia can activate Rac1 suggest that RhoA is an upstream activator of Rac1 at the leading edge¹². However, RhoA can also inhibit Rac1 through its effector Rho kinase, which can activate several GAPs (ArhGAP22 and FilGAP) that inactivate Rac1.¹³⁻¹⁵ Likewise, Rac1 through its downstream effectors can either inhibit or activate RhoA, depending on the cell context and spatial localization.^{11,16-18} In addition through its effector mDia1, RhoA can activate its own GEF (LARG), thereby generating an auto-activation loop.¹⁹ These positive and negative protein interaction loops in GTPase cascades can bring about complex spatiotemporal dynamics, including all-or-none switches, oscillations and intricate spatial patterns.^{18,20-24} Even a seemingly simple system of only two GTPases with an auto-activation loop and reciprocal influences of GTPases (feedforward activation and feedback inhibition), which resembles the RhoA/Rac1 cascade, was shown to potentially exhibit three distinct dynamic behaviors: (i) abrupt, bistable switches, (ii) excitable behavior, and (iii) sustained oscillations.²⁵

RhoA and Rac1 shuttle between the cell membrane and the cytoplasm, and in the cytoplasm RhoA and Rac1 are sequestered by the cytosolic RhoGDIs.²⁶ When these GDIs bind to GDP-bound forms of the GTPases, GDIs inhibit the dissociation of GDP and prevent GTPase activation by GEFs. If GDIs bind a GTP-bound form of the GTPase, all interactions with GTPase effectors are inhibited, precluding any biological activity of this GTPase. Thus, the inhibitory role of GDIs in regulating the GTPase activities is well understood and appreciated.²⁶ However, recent experimental findings suggest more complex functions of GDIs. The GTPase-GDI complexes can be regulated by different proteins, including kinases which phosphorylate GTPases and GDIs, leading to dramatic changes in the binding affinities.²⁷ These phosphorylation-induced changes can either cause tighter binding of a GDI and a GTPase resulting in an inert complex, or on the contrary to the release of the GTPase from the complex and subsequent association with the membrane.^{27,28} Yet, how this phosphorylation-mediated regulation of the RhoGDI affinity for the Rho-family GTPases affects the RhoA/Rac1 cascade dynamic responses is poorly understood.

The present paper uses a dynamic modeling approach to show that GDIs are not merely GTPase inhibitors, but dedicated controllers of the intricate spatiotemporal behavior of the Rho-family GTPases. We demonstrate that the GDI/GTPase ratio and the GDI-GTPase binding affinities are critical regulators of the GTPase cascade dynamics. We show that the RhoA/Rac1 cascade, which is controlled by interactions with RhoGDIs, can exhibit bistable, oscillatory and excitable dynamics, and further that this RhoGTPase system can be driven into the distinct behavioral modes solely by changing the RhoGDI abundances or their affinities for GTPases. These different dynamic

modes of RhoA and Rac1 activities and their regulation by RhoGDI form the basis of protrusion-retraction cycles at the leading edge of migrating cells.

Results

Building a computational model of the RhoA/Rac1 cascade regulated by GDIs.

In order to elucidate the effects of the GDIs on the GTPase cascade dynamics, we built a computational model comprised of nonlinear ordinary differential equations (ODEs). These ODEs are a mathematical representation of the system, exactly describing how the concentrations of active RhoA and Rac1 and their complexes with GDI change over time. The model can be used to simulate the system response to stimuli or changes in the parameters, such as the GTPase and GDI abundances and the GDI affinity for GTPases, thus providing a convenient tool to explore the system dynamics and generate predictions that can be compared with the reported experimental observations or tested against the experiment.

Our model focuses on the cascade of the two GTPases, RhoA and Rac1, and incorporates their interactions with RhoGDI. Based on the experimental data, we assume that there are mutual activating and inhibiting interactions between these GTPases and also an auto-activation loop for one GTPase. Both activation and inhibition can be represented by different molecular mechanisms. For instance, inhibition of RhoA by Rac1 can arise from either inhibition of a GEF for RhoA or activation of a GAP for RhoA, whereas RhoA auto-activation can be brought about by RhoA-induced activation of its own GEF or inhibition of its GAP. Thus, the same kinetic influence diagram of the RhoA/Rac1 cascade (Fig. 1a) corresponds to $2^3 = 8$ different molecular interaction circuits²⁵. Importantly, we recently demonstrated that 8 different cascade circuitries, which present all possible molecular realizations of a particular kinetic influence scheme, display the same number of steady states and similar dynamics in both time and space (see also Supplementary Information 1 (SI 1)).²⁵ Therefore, for illustrative purposes in the main text we assumed that mutual activating and inhibitory interactions affect only GEF mediated GDP/GTP exchanges. This assumption does not change the potential variety of dynamics displayed by the RhoA/Rac1 cascade (see SI1 where the same influence diagram of RhoA/Rac1 interaction is implemented in terms of an alternative cascade circuitry where RhoA inhibition by Rac1 is mediated by activation of GAPs for RhoA).

RhoGDI1 is the most ubiquitously expressed member of RhoGDI family, and it interacts with several RhoGTPases including RhoA and Rac1.²⁹ Recent evidence suggests that while RhoGTPases cycle between the membrane and the cytoplasm, some elementary processes of the RhoGTPase dissociation from the membrane and their association with the membrane can be GDI-independent, whereas the other trafficking reactions can depend on GDIs for diverse pathways and conditions.³⁰⁻³³ Since in the cytoplasm GTPases rapidly bind to GDIs, in the model we consider the overall reactions where the dissociation of a GTPase from the membrane is combined with the binding to a GDI, and the dissociation of a GTPase from the GDI is combined with the subsequent membrane association. In terms of the overall reactions, the data show that the GTP-bound RhoGTPase binds GDIs with much lower affinity than the GDP-bound RhoGTPase²⁸ (in line with the observations that the latter dissociates much faster from the membrane than the former).^{30, 31} While this difference in the equilibrium affinity constants is included in our model, it is unknown if the affinities of RhoGDI1 for RhoA and Rac1 are similar or significantly different. Thus in the model GDI – GTPase interactions are described by the mass action kinetics, and the affinities for both GTPases are assumed similar (See Table 1 in SI).

A kinetic description

We consider a two layer RhoGTPase cascade (Fig. 1b) and denote by G_1P and G_2P the

active concentrations of the GTPases at the first and second layers, respectively. At each cascade layer at the membrane, a GEF catalyzes a transition of a GTPase from its inactive GDP-bound form (G_i) to its active GTP-bound form (G_iP), while a GAP catalyzes the reverse process (G_iP transformation into G_i). The RhoGDI (denoted by I) can bind to both active and inactive GTPase forms. The GDI binding sequesters the GTPase away from the membrane, rendering the cytoplasmic complexes (G_1I, G_1PI, G_2I, G_2PI), which are inactive (Fig. 1b). On the time scale considered, the total concentration of inactive, active and bound to GDI forms is conserved for each GTPase (see Eq. 1 in Methods).

As mentioned above, considering RhoA and Rac1 as a prototypic example, we assume that G_1P activates G_2P , whereas G_2P inhibits G_1P , and G_1P also activates itself through an auto-regulatory loop mediated by its own GEF. For simplicity, we assume that the rates of GEF and GAP-catalyzed reactions can be described by the Michaelis-Menten expressions where the regulatory influences of GTPases on GEFs and GAPs correspond to pure non-competitive mechanisms of enzyme inhibition or activation.^{25,34} This allows us to present any reaction rate (u_j , $i = 1 - 4$) as the product of the Michaelis-Menten rate (in the absence of regulatory interactions) and modifying, dimensionless multipliers, $\alpha_{ij}(G_iP)$, which specify the auto-regulatory, feedforward or feedback influence of G_iP on the rate u_j (Eqs. 2 and 3 in Methods). Each multiplier $\alpha_{ij}(G_iP)$ is described by a Michaelis-Menten type function of the corresponding active GTPase fraction,^{25,34} where the maximal degree of activation or inhibition is determined by the coefficient a_{ij} . An $a_{ij} > 1$ indicates activation; $a_{ij} < 1$ inhibition; and $a_{ij} = 1$ indicates the absence of regulatory interactions, in which case the modifying multiplier $\alpha_{ij}(G_iP)$ equals 1 (Eqs. 3 in Methods). Finally, GDI-GTPase binding reactions are denoted u_{ci} , $i = 1 - 4$, and are based on the standard mass action kinetics. The temporal dynamics of RhoA/Rac1 cascade is governed by the system of ODEs presented in Eqs. 2. For convenience, we use the normalized (dimensionless) concentrations of GTPases g_1, g_1p, g_2, g_2p and their respective GDI complexes g_1I, g_1pI, g_2I, g_2pI , which represent GTPase fractions, i.e. $g_1 = G_1/G_1^{tot}$ and $g_2pI = G_2PI/I^{tot}$. For a complete description of the normalized ODE system, we refer to Eqs 4 – 7 in Methods.

Parameter values. Available experimental data show wide ranges of kinetic parameters for the GTPase - GDI system and warrant a detailed exploration of Rac1 and RhoA responses under various conditions that encompass the vast parameter space. The data suggest that the total amount of RhoGDI is roughly in the same range as the sum of the RhoGTPase abundances.^{29,35} We varied the GDI/GTPase ratio from 0 to 2. The affinities for the GDI-GTPase binding were informed by available data in the literature (see Supplementary Information). As mentioned above because of the lack of the available data, RhoGDI1 affinities for both RhoA and Rac1 are assumed to be similar, whereas the affinities for inactive GDP-bound forms are set higher than the affinities for active GTP-bound forms, as reported in the literature.^{28,36}

Intricate temporal dynamics of the Rac1/RhoA cascade

A cascade of two interacting Rho-family GTPases and RhoGDI1 can exhibit bistable switches, sustained oscillations and excitable, overshooting transitions.

The positive and negative interactions in the RhoA/Rac1 cascade regulated by GDIs generate a variety of distinct dynamic behaviors ranging from bistable switches to excitable pulses and sustained oscillations. Here we first briefly characterize each of the observed behaviors and further describe how GDI regulates the GTPase cascade dynamics.

Bistable behavior of GTPase cascades. Bistability is a recurrent motif of a variety of

biological systems, including CDK/Cdc2/Cyclin B and MAPK cascades.³⁷⁻⁴⁰ A bistable system can switch between two distinct stable steady states, and is unable to reside in the intermediate, unstable state. Generally, such behavior in GTPase cascades arises from the presence of a positive feedback loop, which in our model is generated by the auto-catalytic activation of RhoA (See Fig. 1a). A characteristic feature of bistable systems is the so called hysteresis effect, implying that the stimulus must exceed a certain threshold in order for the system to switch to a different steady state at which it will reside even if the stimulus decreases. For example, once the stimulus resulting in the increase in GEF1 activity exceeds the threshold ($r_{\text{GEF1}} = P_1$, where r_{GEF1} is normalized GEF1 activity, see Methods,) it causes the abrupt switch “on” of both GTPase activities (Fig. 2a, the P_1 threshold is called turning point). In order to come back to the initial “off” state, the stimulus must decrease below the other threshold value corresponding to the turning point P_2 . For GEF1 concentrations in between the thresholds (i.e. $P_1 < r_{\text{GEF1}} < P_2$) the system can reside in either the "on" or the "off" state depending on its history. Remarkably, bistability is not the only behavior in the model and a steady increase in the ratio of the GDI and GTPase abundances (GDI/GTPase ratio) can lead to an entirely different GTPase dynamics.

Excitable pulses of GTPase activity. In addition to bistability, the RhoA/Rac1 cascade regulated by GDI can exhibit excitable behavior, which resembles the dynamics of classic excitable systems, such as action potential in neurons or heart Purkinje fibers.^{41, 42} Excitable models can be divided into two types depending on their response to the stimulus.⁴³ Type I models show ‘all-or-nothing behavior’ which consist of either a significant pulse or a simple decay to the steady state. Hence, a Type I excitable system responds to stimuli with either low or high amplitude, whereas there are no intermediate responses, merely proportional to the stimulus. On the other hand, in the Type II models, the amplitude of the response is continuously proportional to the perturbing stimulus.⁴³ Here, the RhoA/Rac1/GDI cascade demonstrates Type I excitability, operating as an excitable digital device with a built-in excitability threshold. Fig. 2b shows Rac1 and RhoA activity responses to a perturbation in the concentration of GEF for RhoA. If the initial perturbation (shown by an arrow at time =10 sec) does not exceed the threshold (at $r_{\text{GEF1}}=5.15$), both GTPase activities rapidly return to their steady state values (the corresponding time courses are shown by dashed lines), whereas for over-threshold perturbations, a large overshoot response occurs before GTPase activities return to the basal state (solid lines). This distinct from Fig. 2a response dynamics is caused by changing only the GDI/GTPase ratio. Thus, a variation of the GDI/GTPase ratio can move the system from the bistable domain to a region where it can exhibit excitable overshoots. Further regulation of the GDI/GTPase ratio transitions the GTPase system to yet another behavior: oscillatory dynamics.

Sustained oscillations in GTPases. Oscillations of GTPase activities have been demonstrated both computationally and experimentally, e.g. oscillations in the active Cdc42, Cdc42 protein and Cdc42 GEF during polarized cell growth in fission yeast.⁴⁴ In the oscillatory regime, the system cannot reside in a steady state and oscillates in a self-perpetuating manner with a constant amplitude and frequency. In general, oscillations can occur in a two GTPase cascade if the cascade is potentially bistable (due to a positive feedback loop), while both GTPases oppositely regulate each other (creating a negative feedback).^{25, 45} This alteration of a negative and a positive feedback ensures that the system is periodically forced to switch from a high to a low state and vice versa. In our model, this oscillatory mechanism is brought about by an auto-activating loop on RhoA and the opposite influence between the two cascades (RhoA activates Rac1, whereas Rac1 inhibits RhoA). This forces the GTPase activities to jump periodically between two distinct states (Fig. 2c).

How changes in the RhoGDI abundance affects RhoA/Rac1 system responses

As evidenced above, all the different dynamics (bistable switches, excitable overshoots and oscillations, Fig. 2a-c) can be brought by solely regulating the GDI/GTPase ratio (denoted by γ). In order to visualize the transitions between these dynamic behaviors, we created so-called bifurcation

diagrams (Fig.S1). These diagrams show how changing the GDI/GTPase ratio drives the model from one distinct dynamic behavior to the next and further at which values precisely these transitions occur (bifurcation points).

When GDI is absent ($\gamma = 0$), RhoA-Rac1 cascade dynamics is in the bistable regime and it stays bistable at low GDI/GTPase ratios (i.e. at $\gamma = 0.05$, Fig. 2a). However, the dynamics of the GTPase system is not bistable everywhere and increasing the GDI/GTPase ratio reaches a point where the dynamic behavior changes abruptly and bistability is lost (which is known as a saddle node bifurcation, Fig. S1). With the further rise in the GDI/GTPase ratio, an excitable behavior emerges. Within the excitable region, GDI increases cause more subtle changes of the GTPase dynamics: excitable pulses occur with a much greater magnitude and time period (Fig. 3a). Additional upregulation of the GDI/GTPase ratio brings the RhoGTPase cascade from the excitable to the oscillatory regime (known as the supercritical Hopf bifurcation, shown by the left HB point in Fig. S1). Increasing the GDI/GTPase ratio within this oscillatory regime increases the amplitude and period of the oscillations (Fig. 3b). Finally, oscillatory regime terminates (the right supercritical Hopf bifurcation point in Fig. S1), leading to the monostable regime. Importantly, the control of GTPase dynamics by GDI is robust, and all three behaviors (bistable, excitable and oscillatory) can be observed for different parameter sets (see example in Fig. S2, where the dynamic GTPase responses of Fig. 2 are compared with the responses for a perturbed parameter set given in Table S2).

Regulation of RhoGTPase dynamics by combined changes in GEFs/GAPs and RhoGDI

We can conveniently describe RhoGTPase activity in relationship to changes in various kinetic parameters by dividing a plane of two selected parameters into the regions, which represent different types of dynamic responses. This partitioning of the parameter space helps us to summarize how changes in GTPase activators and inhibitors and the RhoGDI abundance affect the activity of GTPases and bring about oscillations, excitable pulses and bistable switches. The different colored regions indicate regions of distinct dynamic behavior depending on the concentrations of GAP1 (Fig. 4a) or GEF1 (Fig.4b) and GDI/GTPase ratio.

The white region occupying most of the plane corresponds to monostable region (points M_i , $i=1-4$) of RhoA activity. Within this region the GTPase system can also display excitable behavior (point E), where pulse responses of high-amplitude occur for any stimulus exceeding a certain threshold (Fig. 2b). The next large area, indicated in pink, corresponds to the oscillatory behavior of the GTPase system. Here, the GTPase activities follow a cyclic perpetual behavior exemplarily shown in Fig. 2c. Finally, bistable switches occur within the grey region.

Moving left to right represents increasing GDI/GTPase ratio, similarly moving in the upward direction corresponds to increasing GAP1 (Fig. 4a) or GEF1 (Fig. 4b) levels. Consequently, the dashed vertical lines in Fig. 4a show what regimes can occur if we upregulate GAP1 at fixed low (the left dashed line) or high (the right dashed line) GDI/GTPase ratios. Here we see that when GDI/GTPase ratio is low ($\gamma = 0.05$), upregulating the GAP1 level can bring about bistable responses in RhoA (Fig.S3a), whereas at the higher GDI/GTPase ratio ($\gamma=0.95$) an oscillatory behavior emerges (Fig. S3b). Similarly, the dashed horizontal lines correspond to the rising GDI/GTPase ratio at constant GAP and GEF levels. Specifically, the horizontal lines in Figs. 4a and 4b illustrate that at fixed levels of GEF and GAP, the RhoGTPase system can first exhibit bistability (point B), then excitable behavior (point E), then oscillations (point O), and finally monostable behavior. Remarkably, this variety of different dynamic responses can never be achieved by GEF or GAP regulation, since crossing vertically can never reach both the bistable and the oscillatory region. Thus, neither changing GEF nor GAP alone can generate the same variety of dynamic behaviors that the GDI regulation does. This conclusion is also corroborated by exploring how the GTPase dynamics is regulated by combined changes in GEF and GAP at the different GDI/GTP ratios set at bifurcation points (Fig. S4).

Regulation of RhoGDI/RhoGTPase binding affinity provides similar qualitative results as changing the RhoGDI/GTPase ratio

The RhoA-Rac1 system can be driven into different modes of dynamic behavior not only by controlling RhoGDI/GTPase ratio, but also by regulating RhoGDI-GTPase affinity. Experimentally, the GTPase-GDI affinities can be controlled by protein kinases, which phosphorylate GTPases and GDIs, leading to dramatic changes in the binding affinities. For instance, phosphorylation of RhoA by protein kinase A (PKA) facilitates RhoA binding to RhoGDI, thereby promoting RhoGDI to associate faster to RhoA and sequester the complex into the cytoplasm.²⁸

Here we controlled the binding affinity by changing the rate constant for binding RhoGDI to RhoA (denoted b_l , see Eq. 4 in Methods). The simulations show qualitative results similar to those obtained by increasing GDI/GTPase ratio, whereby the GTPase cascade dynamics change in the same particular order: from bistable, to excitable, to oscillatory to monostable (Fig. S5).

Our theoretical findings are in line with recent experimental observations that demonstrate the regulation of the GTPase dynamics and cell migration by RhoGDIs. In particular, protrusion-retraction cycles in migrating cells are shown to be affected by RhoGDI expression levels and RhoGDI affinity for RhoA.²⁸ Overexpressing RhoGDI enhanced cellular migration and decreased the duration of the protrusion cycle, while increasing the affinity of RhoGDI to RhoA resulted in smaller amplitudes of protrusions.²⁸ Similarly, our simulation results show that downregulation of the RhoGDI level increases the duration cycle of both the excitable and oscillatory pulses (Fig. 3).

An alternative model of Rac1 mediated activation of RhoA-GAP yields the same qualitative results as Rac1 mediated inhibition of RhoA-GEF

The analysis presented above is based on the kinetic scheme shown in Fig. 1b. However for the same influence diagram (Fig. 1a), experimental evidence suggest that Rac1 can inhibit RhoA by either (1) inhibiting RhoA-GEFs (p115⁴⁶ and GEF-H1^{33, 44, 47}) or (2) activating a RhoA-GAP (p190RhoGAP)^{31, 48}. Our analysis so far considered the first possible mechanism of GEF-mediated inhibition. To account for the second inhibitory mechanism, we built a model where Rac1 activates RhoA hydrolysis (Fig. S6). Not surprisingly, both models behave similarly (See model responses in Figs. S7 and S8 at different GDI-RhoA association parameters and different GDI/GTPase ratios respectively), which is in agreement with our previous findings.²⁵ As for GEF-mediated inhibition, the increase in the GDI/GTPase ratio and the GDI-GTPase affinity in the second model (Fig. S6) drives the system dynamics through bistable, excitable and oscillatory regimes (Fig. S9). Thus, both models yield the same qualitative results. We conclude that the outcome of GDI regulation is largely independent of mechanistic details of molecular circuitry, provided that the overall interaction topology remains the same (Fig. 1a).

Discussion

Cellular behavior depends on the precise control of protein activities. To achieve specific biological functions, these activities are coordinated by complex interaction networks featuring multiple feedback loops. Complex dynamic behaviors emerge in these signaling systems, including all-or-none responses and hysteresis driving specific cell fate decisions, for instance, the synchronization of oscillators in the circadian rhythm and the encoding of information in the frequency of p53 pulses during the DNA damage response.^{8, 49-51} Although the signal processing functions of many cellular systems, for instance kinase/phosphatase cascades, are well recognized⁵²⁻⁵⁴, a detailed understanding of small GTPase networks is largely missing. It is known that GTPase cascades can exhibit complex spatiotemporal dynamics, but how the cell controls the different dynamic behaviors and how GDIs are involved in this regulation is largely unknown.^{21-25, 45} To address this question, we constructed mathematical models of the interactions between RhoA, Rac1

and RhoGDI at the leading edge of migrating cells. Featuring a positive and a negative feedback loop, this system is particularly rich in terms of the different dynamic behaviors it can generate. Recently, the term “frustrated bistability” was coined for circuitry containing positive feedback that brings about bistability together with a destabilizing negative feedback that transforms a bistable behavior into sustained oscillations.^{45,55} These oscillations generally do not have sinusoidal shapes and are referred to as relaxation oscillations.

We demonstrate that the regulation of the GDI abundance or the GDI affinities for RhoA and Rac1, transition the system from bistable to excitable and then to oscillatory and monostable behaviors. Importantly, neither regulating GEF nor GAP can yield the same dynamic variety. Our analyses suggest that regulating GDI provides efficient means of controlling the different GTPase dynamics and associated biological processes.

RhoGTPases coordinate the protrusion-retraction cycle of migrating cells, and the experimentally monitored activity patterns of RhoA and Rac1^{11,56} can be explained by the oscillatory and excitable dynamics observed in our model. Further, it was suggested that RhoA and Rac1 can function as master regulators that can switch cells between distinct modes of cell migration (e.g. amoeboid versus mesenchymal).^{18,57} For example, migration of growth factor stimulated cells is characterized by high, stable Rac1 activity, whereas fibronectin-induced membrane protrusions exhibit oscillatory RhoA dynamics.^{56,58} It was reported that the GTPase functions differ for distinct subcellular locations, such as the leading edge and the rear, and the different spatiotemporal GTPase modules are highly organized and talking to each other.¹⁸ Although our model suggests that the modulation by RhoGDI can switch the RhoA/Rac1 GTPase system between different modes of action, it remains to be proven experimentally how much of the apparent differences can indeed be explained by the regulation of GDIs. A recent report showing that dramatic changes of the RhoGDI affinity for RhoA induced by PKA-mediated RhoA phosphorylation govern the oscillations of RhoA activity at the leading edge of migrating cells supports our modeling conclusions and further suggest that RhoGDI is part of a RhoA negative feedback loop involving PKA.²⁸

Generally, the GDI-GTPase interactions are themselves highly regulated by a variety of mechanisms.²⁹ First, a variety of proteins compete with GDIs for binding to RhoGTPases thus acting as GDI displacement factors (GDF). Ezrin, radixin and moesin but also the neurotrophin receptor p75NTR are such examples. Second, phosphorylation can regulate the GDI-GTPase affinity. Generally the phosphorylation RhoGTPases promotes their association with RhoGDI, whereas the phosphorylation RhoGDI promotes their dissociation. Our analysis provides theoretical evidence that this regulation of the GDI-GTPase interaction provide efficient means for the cell to switch GTPase signaling between different modes of dynamic behaviors. Such switches may be of particular importance in situations where cells have to dynamically adapt to changing environmental condition as occur during cell migration. An interesting variation on this theme is to consider a spatially inhomogeneous distribution of GDIs within the cell, which could evoke different RhoA/Rac1 dynamics in different subcellular compartments. Thus, the addition of GDIs to GTPase signaling networks seems much more than a dull protein sequestration mechanism, by conveying a rich dynamic behavior. However, further experimental studies are necessary to confirm this prediction and determine whether and which GTPase systems actually employ the here described mode of regulation.

Materials and methods

Kinetic equations describing the RhoA/Rac1/RhoGDI1 interaction model

We consider a time scale on which the concentrations of both GTPases and GDI are conserved, thus:

$$G_1 + G_1P + G_1I + G_1PI = G_1^{tot},$$

$$\begin{aligned}
G_2 + G_2P + G_2I + G_2PI &= G_2^{tot}, \\
I + G_1I + G_1PI + G_2I + G_2PI &= I^{tot}.
\end{aligned} \tag{1}$$

We denote by G_1P and G_2P the active concentrations of the first and second GTPases, respectively. The GDI (denoted by I) can bind to both active GTP bound and inactive GDP bound forms. Denoting the reaction rates of GTPase activation and deactivation by u_1, u_2, u_3, u_4 and GDI binding rates by $u_{c1}, u_{c2}, u_{c3}, u_{c4}$ (Fig. 1b), the temporal dynamics of the two layered GTPase cascade can be described by the following system of ODEs:

$$\begin{aligned}
\frac{dG_1}{dt} &= -u_1 + u_2 - u_{c1}, \\
\frac{dG_1P}{dt} &= u_1 - u_2 - u_{c2}, \\
\frac{dG_2}{dt} &= -u_3 + u_4 - u_{c3}, \\
\frac{dG_2P}{dt} &= u_3 - u_4 - u_{c4}, \\
\frac{dG_1I}{dt} &= u_{c1}, \\
\frac{dG_1PI}{dt} &= u_{c2}, \\
\frac{dG_2I}{dt} &= u_{c3}, \\
\frac{dG_2PI}{dt} &= u_{c4}, \\
u_1 &= \alpha_{11}\alpha_{21}V_1 \frac{G_1/K_1}{1 + G_1/K_1}, \\
u_2 &= V_2 \frac{G_1P/K_2}{1 + G_1P/K_2}, \\
u_3 &= \alpha_{13}V_3 \frac{G_2/K_3}{1 + G_2/K_3}, \\
u_4 &= V_4 \frac{G_2P/K_4}{1 + G_2P/K_4}, \\
u_{c1} &= p_1 \cdot I \cdot G_1 - d_1 \cdot G_1I, \\
u_{c2} &= p_2 \cdot I \cdot G_1P - d_2 \cdot G_1PI, \\
u_{c3} &= p_1 \cdot I \cdot G_2 - d_1 \cdot G_2I, \\
u_{c4} &= p_2 \cdot I \cdot G_2P - d_2 \cdot G_2PI.
\end{aligned} \tag{2}$$

Here the parameters V_i are the maximal rates of GEF and GAP catalyzed reactions, and K_i are the corresponding Michaelis constants. The parameters p_1, p_2 and d_1, d_2 denote association and dissociation constants of GDI - GTPase interactions, respectively. Dimensionless multipliers α_{ij} are the mutual GTPase interactions, where i corresponds to the GTPase (G_iP) and j denotes the reaction rate (u_j) which is influenced by G_iP . Thus, α_{11} describes the auto-regulatory loop of the first cascade, and α_{13}, α_{21} describe activating and inhibiting reactions mediated by the first and second GTPase, respectively (See Fig. 1b). Assuming general hyperbolic modifier kinetics, activation/inhibition strengths a_{ij} can be described as follows,

$$\alpha_{ij}(g_i p) = \frac{1 + a_{ij}G_iP/K_{ij}}{1 + G_iP/K_{ij}}. \tag{3}$$

Here K_{ij} denotes activation or inhibition constants and a_{ij} denotes an activation/inhibition parameter, where $a_{ij} > 1$ is activation and $0 < a_{ij} < 1$ is inhibition.

For convenience we normalize the ODE system introduced in (2):

$$\begin{aligned}
\frac{dg_1}{dt} &= -v_1 + v_2 - \gamma \cdot v_{c1}, \\
\frac{dg_1p}{dt} &= v_1 - v_2 - \gamma \cdot v_{c2}, \\
\frac{dg_2}{dt} &= -v_3 + v_4 - \gamma \cdot v_{c3}, \\
\frac{dg_2p}{dt} &= v_3 - v_4 - \gamma \cdot v_{c4}, \\
\frac{dg_1I}{dt} &= v_{c1}, \\
\frac{dg_1pI}{dt} &= v_{c2}, \\
\frac{dg_2I}{dt} &= v_{c3}, \\
\frac{dg_2pI}{dt} &= v_{c4}, \\
v_1 &= \alpha_{11}\alpha_{21}r_{GEF1} \frac{g_1/m_1}{1 + g_1/m_1}, \\
v_2 &= r_{GAP1} \frac{g_1p/m_2}{1 + g_1p/m_2}, \\
v_3 &= \alpha_{13}r_{GEF2} \frac{g_2/m_3}{1 + g_2/m_3}, \\
v_4 &= r_{GAP2} \frac{g_2p/m_4}{1 + g_2p/m_4}, \\
v_{c1} &= b_1 \cdot f \cdot g_1 - d_1 \cdot g_1I, \\
v_{c2} &= b_2 \cdot f \cdot g_1p - d_2 \cdot g_1pI, \\
v_{c3} &= b_1 \cdot f \cdot g_2 - d_1 \cdot g_2I, \\
v_{c4} &= b_2 \cdot f \cdot g_2p - d_2 \cdot g_2pI \quad (4)
\end{aligned}$$

with the following normalizations:

$$\begin{aligned}
g_1 &= G_1/G_1^{tot}, g_1p = G_1P/G_1^{tot}, g_2 = G_2/G_2^{tot}, g_2p = G_2P/G_2^{tot}, \\
g_1I &= G_1I/I^{tot}, g_1pI = G_1PI/I^{tot}, g_2I = G_2I/I^{tot}, g_2pI = G_2PI/I^{tot}, f = I/I^{tot}, \\
\gamma &= I^{tot}/G_1^{tot} = I^{tot}/G_2^{tot}, b_1 = p_1 \cdot G_1^{tot} = p_1 \cdot G_2^{tot}, b_2 = p_2 \cdot G_1^{tot} = p_2 \cdot G_2^{tot}, \\
m_1 &= K_1/G_1^{tot}, m_2 = K_2/G_1^{tot}, m_3 = K_3/G_2^{tot}, m_4 = K_4/G_2^{tot}, \\
r_{GEF1} &= V_1/G_1^{tot}, r_{GAP1} = V_2/G_1^{tot}, r_{GEF2} = V_3/G_2^{tot}, r_{GAP2} = V_4/G_2^{tot}. \quad (5)
\end{aligned}$$

Normalized parameters m_i are the ratios of Michaelis constants and the total GTPase expressions and r_{GEFi} , r_{GAPi} ($i = 1-2$) are dimensionless maximal rates (normalized by total GTPase abundances). Mutual interaction scheme between G_i and G_j is specified by normalized multipliers α_{ij} :

$$\alpha_{ij}(g_i p) = \frac{1 + a_{ij}g_i p/m_{ij}}{1 + g_i p/m_{ij}} \quad (6)$$

where indices i and j describe the influence of $g_i p$ on the enzyme reaction v_j . Parameters m_{ij} denote

Michaelis-Menten-type half-activation/half-inhibition constants, and a_{ij} denote the levels (or strengths) of activation/inhibition. Thus, α_{11} with $\alpha_{11} > 1$ describes an auto activating regulatory loop mediated by G_1 , and α_{13} with $\alpha_{13} > 1$ and α_{21} with $0 < \alpha_{21} < 1$ denotes mutual activating and inhibiting interactions, respectively.

In (4) GDI binding rates are described by v_{c1}, v_{c2}, v_{c3} and v_{c4} and assume mass action kinetics. The model assumes that GDI is nonspecific for both GTPases and can bind to inactive/active forms with the same affinities. Also the ratios of total concentration of the GDI to the total abundances of the two GTPases are assumed to be equal (i.e. $I^{tot}/G_1^{tot} = I^{tot}/G_2^{tot}$) and are denoted by γ .

Finally, conserved moieties in (1) are normalized by the corresponding GTPase and GDI concentrations:

$$\begin{aligned} g_1 + g_1p + \gamma \cdot g_1I + \gamma \cdot g_1pI &= 1 \\ g_2 + g_2p + \gamma \cdot g_2I + \gamma \cdot g_2pI &= 1 \\ i + g_1I + g_1pI + g_2I + g_2pI &= 1 \end{aligned} \quad (7)$$

The normalized conserved moieties allow to eliminate for inactive forms of G_1 and G_2 (denoted g_1, g_2) as well as for the free form of GDI (denoted f) in (4) and lead to the system of ODEs, which is used to explore the dynamics of the model.

Acknowledgement We thank Alexander von Kriegsheim for discussions. Supported by Science Foundation Ireland under Grant No. 06/CE/B1129 and PRIMES project under grant agreement number FP7-HEALTH-2011-278568.

Conflict of Interest The authors do not have any competing commercial interests.

Notes and References Electronic Supplementary Information (ESI) is available on the Journal website.

Figures

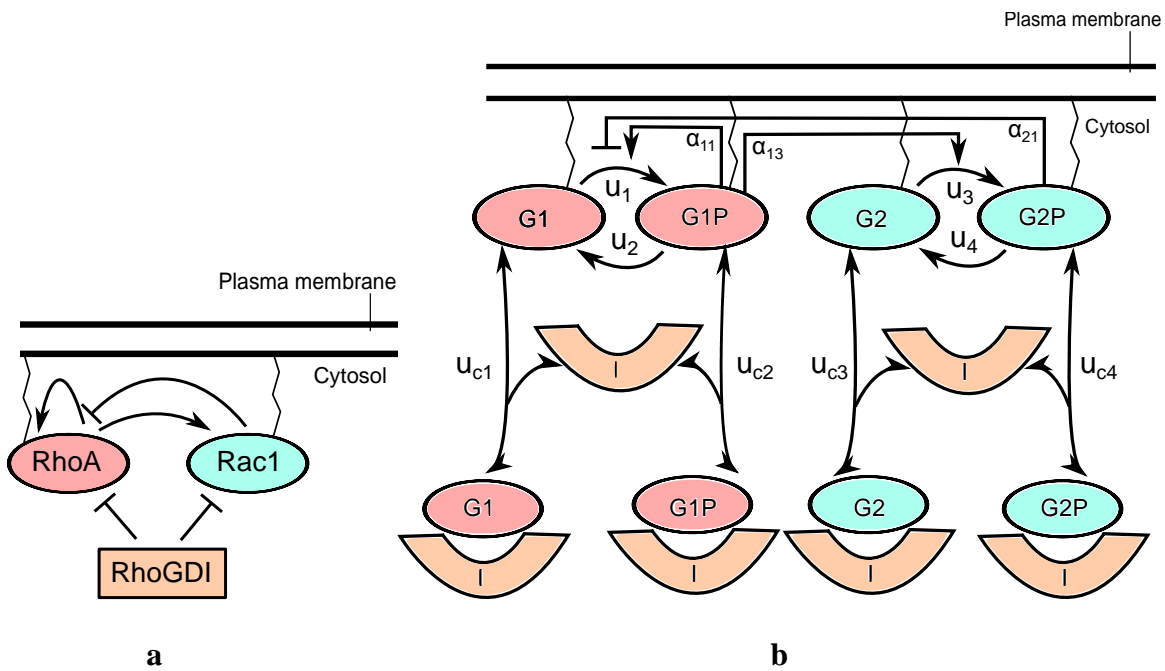


Fig. 1. Kinetic scheme of the GTPase-GDI model. (a) A GTPase cascade interaction structure, called the influence diagram. RhoA activates Rac1 and also activates itself, creating an auto-regulatory loop, whereas Rac1 inhibits RhoA. RhoGDI binds and inhibits both GTPases. (b) Detailed molecular interaction scheme. G_1 and G_2 correspond to the inactive states, and G_1P and G_2P correspond to the active states of RhoA and Rac1, respectively. GEF and GAP catalyzed reactions are denoted by u_i (i denotes a reaction number), which are modified by activating and inhibiting interactions (indicated by α_{ij}). The model assumes that RhoGDI (denoted I) binds to both the inactive and active forms of both RhoGTPases (the corresponding rates u_{c1} , u_{c2} , u_{c3} , u_{c4} are shown) producing inactive complexes in the cytosol.

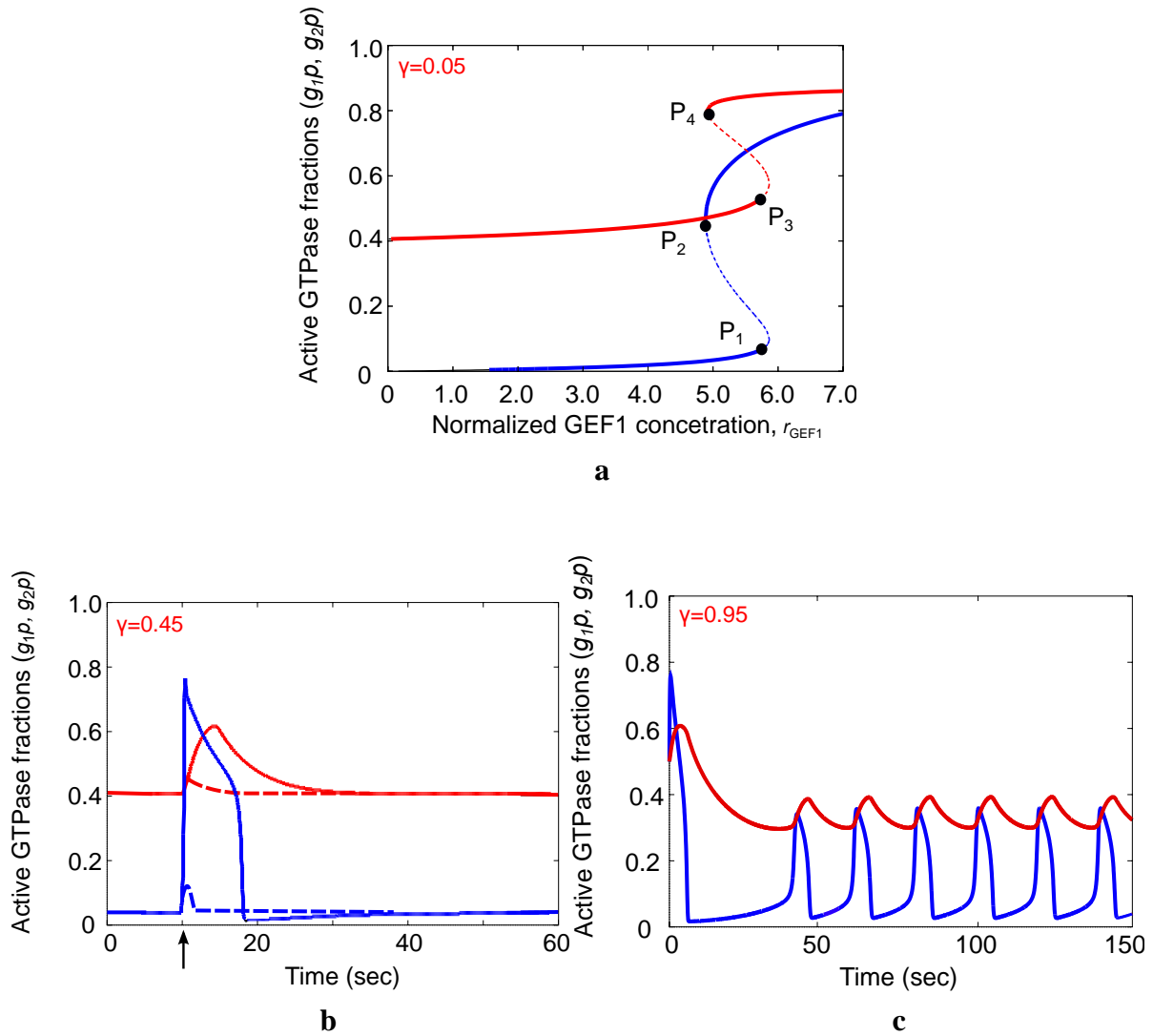


Fig. 2. Bistable, oscillatory and excitable behaviors of RhoGTPases. Responses of active GTPase fractions, g_{1p} (blue) and g_{2p} (red) at different GDI/GTPase ratios (shown in the upper left corner) and at fixed kinetic parameters given in Table 1 in the SI. (a) Bistability and hysteresis in response to changing GEF1 activity. The values of the stable (solid lines) and unstable steady states (dotted lines) are shown for different GEF1 activities. Both active RhoA and active Rac1 fractions are bistable between the turning points (P_1, P_2) and (P_3, P_4) respectively. (b) Excitable overshoot transitions. Initially, a cascade resides in a stable, but excitable steady state. At time $t = 10$ s (marked by black arrow on the time axis), the activity of GEF1 (r_{GEF1}) of the active GTPase at the first layer is perturbed for 1 second. The threshold for excitable pulse is at $r_{GEF1}=5.15$. Sub-threshold perturbations result in responses rapidly returning to the basal steady state (shown by dashed lines). Over-threshold perturbations result in large overshoot responses where the activity of both GTPase fractions markedly increases before returning to the (basal) steady state (c) Sustained oscillations of active GTPase fractions.

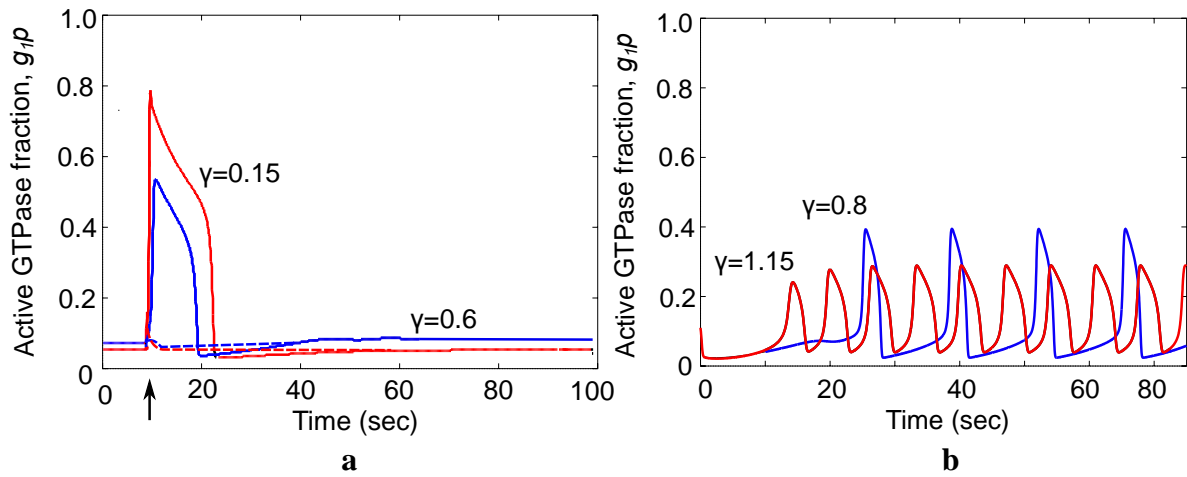


Fig. 3. Qualitative changes in excitable and oscillatory behaviors of GTPases for small changes of the GDI/GTPase ratios. (a) Significant decrease in the duration and magnitude of the overshoot activity in response to increase in the GDI/GTPase ratio (γ) from 0.15 to 0.6. (b) Decrease in the amplitude and period of oscillations caused by increase in γ from 0.8 to 1.15. The values of all other parameters were held constant at the levels given in Tab. S1.

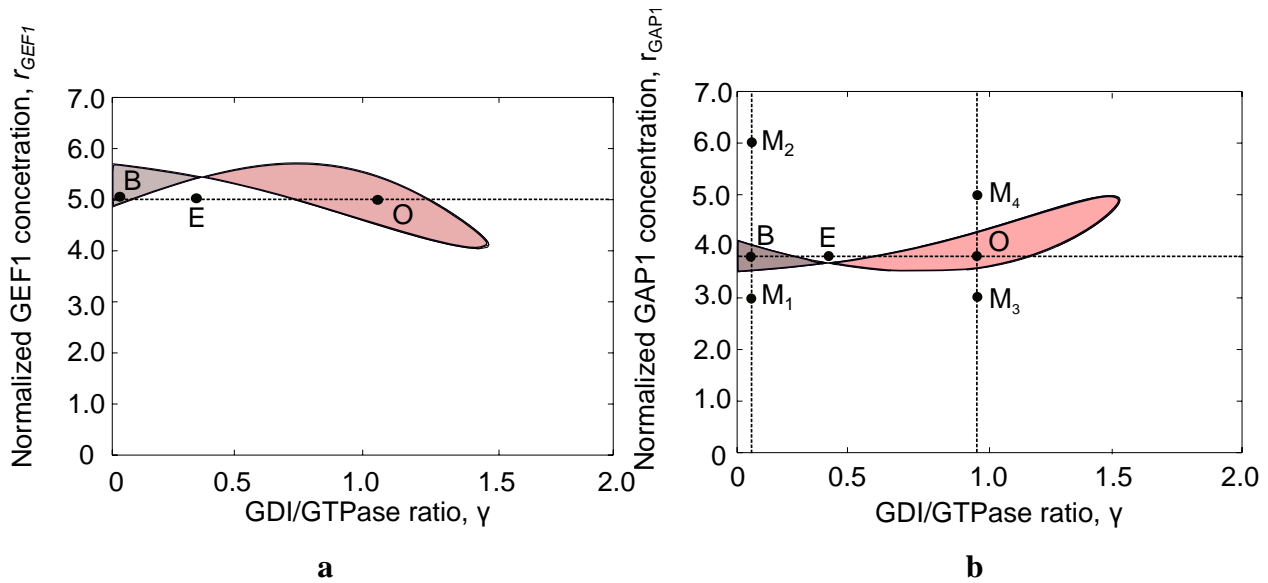


Fig. 4. Separation of the parameter space into regions of qualitatively different behaviors. For different GDI/GTPase ratio (γ) and GAP1 (a) or GEF1 (b) abundances, the parameter space is divided into three regions of qualitatively distinct behaviors: monostable and excitable region (white), bistable region (grey) and oscillatory region (pink). Vertical dashed lines show how increasing GAP1 level at fixed γ can bring different types of GTPase behavior. These lines correspond to one-parameter bifurcation diagrams in Fig. S3a (left line) and Fig. S3b (right line). Similarly, the horizontal dashed lines show how the GDI/GTPase ratio controls RhoGTPase dynamics, corresponding to Fig. S1. The points on the lines mark different regimes such as monostable (M_i , $i = 1-4$), excitable (point E), bistable (point B) and oscillatory (O). The same points are also indicated in the corresponding bifurcation diagrams in Fig. S3.

References

1. Y. Takai, T. Sasaki and T. Matozaki, *Physiol Rev*, 2001, **81**, 153-208.
2. A. J. Ridley, *Journal of cell science*, 2001, **114**, 2713-2722.
3. A. Maciag, G. Sithanandam and L. M. Anderson, *Carcinogenesis*, 2004, **25**, 2231-2237.
4. M. Parri and P. Chiarugi, *Cell Commun Signal*, 2010, **8**, 23.
5. E. Giniger, *Differentiation*, 2002, **70**, 385-396.
6. D. J. Mackay and A. Hall, *The Journal of biological chemistry*, 1998, **273**, 20685-20688.
7. J. Stelling and B. N. Kholodenko, *J Math Biol*, 2008.
8. B. N. Kholodenko, J. F. Hancock and W. Kolch, *Nature reviews. Molecular cell biology*, 2010, **11**, 414-426.
9. S. J. Heasman and A. J. Ridley, *Nature reviews. Molecular cell biology*, 2008, **9**, 690-701.
10. K. A. Felmet, M. W. Hall, R. S. Clark, R. Jaffe and J. A. Carcillo, *J Immunol*, 2005, **174**, 3765-3772.
11. M. Machacek, L. Hodgson, C. Welch, H. Elliott, O. Pertz, P. Nalbant, A. Abell, G. L. Johnson, K. M. Hahn and G. Danuser, *Nature*, 2009, **461**, 99-103.
12. K. Kurokawa and M. Matsuda, *Molecular biology of the cell*, 2005, **16**, 4294-4303.
13. S. Fujioka, K. Yamamoto, R. Okamoto, M. Miyake, K. Ujike, N. Shimada, R. Terada, Y. Miyake, H. Nakajima, C. Y. Piao, Y. Iwasaki, M. Tanimizu and T. Tsuji, *Endoscopy*, 2002, **34**, 318-321.
14. Y. Ohta, J. H. Hartwig and T. P. Stossel, *Nat Cell Biol*, 2006, **8**, 803-814.
15. T. Otomo, C. Otomo, D. R. Tomchick, M. Machius and M. K. Rosen, *Molecular cell*, 2005, **18**, 273-281.
16. E. E. Sander and J. G. Collard, *Eur J Cancer*, 1999, **35**, 1905-1911.
17. K. Burrridge and K. Wennerberg, *Cell*, 2004, **116**, 167-179.
18. O. Pertz, *Journal of cell science*, 2010, **123**, 1841-1850.
19. T. M. Kitzing, A. S. Sahadevan, D. T. Brandt, H. Knieling, S. Hannemann, O. T. Fackler, J. Grosshans and R. Grosse, *Genes Dev*, 2007, **21**, 1478-1483.
20. J. R. Kim, Y. Yoon and K. H. Cho, *Biophysical journal*, 2008, **94**, 359-365.
21. Y. Mori, A. Jilkine and L. Edelstein-Keshet, *Biophysical journal*, 2008, **94**, 3684-3697.
22. Y. Sakumura, Y. Tsukada, N. Yamamoto and S. Ishii, *Biophysical journal*, 2005, **89**, 812-822.
23. P. Del Conte-Zerial, L. Bruschi, J. C. Rink, C. Collinet, Y. Kalaidzidis, M. Zerial and A. Deutsch, *Mol Syst Biol*, 2008, **4**, 206.
24. A. Jilkine, A. F. Mearns and L. Edelstein-Keshet, *Bull Math Biol*, 2007, **69**, 1943-1978.
25. M. A. Tsyanov, W. Kolch and B. N. Kholodenko, *Mol Biosyst*, 2012, **8**, 730-743.
26. C. DerMardirossian and G. M. Bokoch, *Trends in cell biology*, 2005, **15**, 356-363.
27. C. DerMardirossian, G. Rocklin, J. Y. Seo and G. M. Bokoch, *Molecular biology of the cell*, 2006, **17**, 4760-4768.
28. E. Tkachenko, M. Sabouri-Ghomi, O. Pertz, C. Kim, E. Gutierrez, M. Machacek, A. Groisman, G. Danuser and M. H. Ginsberg, *Nat Cell Biol*, 2011, **13**, 660-667.
29. R. Garcia-Mata, E. Boulter and K. Burrridge, *Nature reviews. Molecular cell biology*, 2011, **12**, 493-504.
30. C. V. Falkenberg and L. M. Loew, *PLoS Comput Biol*, 2013, **9**, e1002831.
31. K. Moissoglu, B. M. Slepchenko, N. Meller, A. F. Horwitz and M. A. Schwartz, *Molecular biology of the cell*, 2006, **17**, 2770-2779.
32. J. L. Johnson, J. W. Erickson and R. A. Cerione, *The Journal of biological chemistry*, 2009, **284**, 23860-23871.
33. B. D. Slaughter, A. Das, J. W. Schwartz, B. Rubinstein and R. Li, *Dev Cell*, 2009, **17**, 823-835.

34. A. Cornish-Bowden, *Portland Press, London*, 1995.
35. D. Michaelson, J. Silletti, G. Murphy, P. D'Eustachio, M. Rush and M. R. Philips, *The Journal of cell biology*, 2001, **152**, 111-126.
36. T. Sasaki, M. Kato and Y. Takai, *The Journal of biological chemistry*, 1993, **268**, 23959-23963.
37. N. I. Markevich, J. B. Hoek and B. N. Kholodenko, *The Journal of cell biology*, 2004, **164**, 353-359.
38. U. S. Bhalla, P. T. Ram and R. Iyengar, *Science*, 2002, **297**, 1018-1023.
39. C. P. Bagowski and J. E. Ferrell, Jr., *Curr Biol*, 2001, **11**, 1176-1182.
40. J. E. Ferrell, Jr., *Curr Opin Cell Biol*, 2002, **14**, 140-148.
41. A. L. Hodgkin and A. F. Huxley, *J Physiol*, 1952, **117**, 500-544.
42. D. Noble, *J Physiol*, 1962, **160**, 317-352.
43. W. M. Kistler and W. Gerstner, *Neural computation*, 2002, **14**, 987-997.
44. M. Das, T. Drake, D. J. Wiley, P. Buchwald, D. Vavylonis and F. Verde, *Science*, 2012, **337**, 239-243.
45. B. N. Kholodenko, *Nature reviews. Molecular cell biology*, 2006, **7**, 165-176.
46. H. Rosenfeldt, M. D. Castellone, P. A. Randazzo and J. S. Gutkind, *J Mol Signal*, 2006, **1**, 8.
47. P. K. Biswas, J. P. Christensen, S. S. Ahmed, A. Das, M. H. Rahman, H. Barua, M. Giasuddin, A. S. Hannan, M. A. Habib and N. C. Debnath, *Emerg Infect Dis*, 2009, **15**, 1931-1936.
48. R. I. Bustos, M. A. Forget, J. E. Settleman and S. H. Hansen, *Curr Biol*, 2008, **18**, 1606-1611.
49. J. G. Albeck, G. B. Mills and J. S. Brugge, *Molecular cell*, 2013, **49**, 249-261.
50. J. E. Purvis and G. Lahav, *Cell*, 2013, **152**, 945-956.
51. A. C. Liu, D. K. Welsh, C. H. Ko, H. G. Tran, E. E. Zhang, A. A. Priest, E. D. Buhr, O. Singer, K. Meeker, I. M. Verma, F. J. Doyle, 3rd, J. S. Takahashi and S. A. Kay, *Cell*, 2007, **129**, 605-616.
52. B. N. Kholodenko and M. R. Birtwistle, *Wiley interdisciplinary reviews. Systems biology and medicine*, 2009, **1**, 28-44.
53. O. E. Sturm, R. Orton, J. Grindlay, M. Birtwistle, V. Vyshemirsky, D. Gilbert, M. Calder, A. Pitt, B. Kholodenko and W. Kolch, *Science signaling*, 2010, **3**, ra90.
54. D. Fey, D. R. Croucher, W. Kolch and B. N. Kholodenko, *Frontiers in physiology*, 2012, **3**, 355.
55. S. Krishna, S. Semsey and M. H. Jensen, *Physical biology*, 2009, **6**, 036009.
56. O. Pertz, L. Hodgson, R. L. Klemke and K. M. Hahn, *Nature*, 2006, **440**, 1069-1072.
57. V. Sanz-Moreno, G. Gadea, J. Ahn, H. Paterson, P. Marra, S. Pinner, E. Sahai and C. J. Marshall, *Cell*, 2008, **135**, 510-523.
58. V. S. Kraynov, C. Chamberlain, G. M. Bokoch, M. A. Schwartz, S. Slabaugh and K. M. Hahn, *Science*, 2000, **290**, 333-337.